Electronic excitation of H_2 by electron impact: Close-coupling calculations using the complex Kohn variational method

Steven D. Parker and C. William McCurdy
Department of Chemistry, Ohio State University, Columbus, Ohio 43210

Thomas N. Rescigno and Byron H. Lengsfield III
Lawrence Livermore National Laboratory, P.O. Box 808, Livermore, California 94550
(Received 17 August 1990)

The complex Kohn variational method is employed in four-state close-coupling calculations to generate integral and differential cross sections for low-energy electron-impact excitation of the $X\,^1\Sigma_g^+ \rightarrow (b\,^3\Sigma_u^+, a\,^3\Sigma_g^+$, and $c\,^3\Pi_u)$ transitions in H_2. The integral cross sections for excitation of the $a\,^3\Sigma_g^+$ and $c\,^3\Pi_u$ states from the ground state are found to be significantly different from earlier two-state calculations. The $a\,^3\Sigma_g^+$ cross sections are also larger than the most recent experimental results. This discrepancy is traced to the behavior of the differential cross sections at scattering angles near 0° and 180°, where measurements have not been carried out. The differential cross sections we find for H_2 are strikingly similar to cross sections for analogous transitions in He. Previous theoretical studies of these transitions in He have also shown the two-state approximation to be inadequate.

I. INTRODUCTION

In several recent studies[1–4] we have implemented the complex Kohn[5] variational method in the investigation of electron-molecule scattering. We presented applications to elastic scattering[5] of electrons from CH_4 and to vibrational excitation and electronic excitations in e^--CH_2O collisions.[4] Besides describing the physics of particular systems, these earlier works and those of others[6–8] raise several issues about the convergence of electronic close-coupling calculations for electron-molecule collisions in general. As the incident energy in an electron-molecule collision is increased toward the ionization energy, an infinite number of channels opens up. Although in many applications we are interested only in the cross sections for excitation from the ground state to low-lying excited states, these cross sections are needed for incident energies well above the excitation threshold so that higher excited states are energetically accessible. The question naturally arises as to how many open channels above the threshold of a given excited state must be included to converge a close-coupling calculation to the point that the cross section for its excitation from the ground state is accurate to within a few percent. Also, one may ask under what conditions states with energies below that of the state in question may be neglected. It is noteworthy that questions about the convergence of close-coupling expansions in electron-atom scattering still pose formidable theoretical problems even for the simplest atomic systems. This work is a preliminary investigation of some of these issues for molecular targets using e^--H_2 inelastic cross sections as test cases.

H_2 has six excited states, three singlets and three triplets, with excitation energies below 13.24 eV. These states, with the exception of the $b\,^3\Sigma_u^+$ state, are diffuse and may be considered the first members of Rydberg series converging to the ground state of H_2^+. A simple argument can be made that coupling between the singlet and triplet manifolds might be expected to be weak, because it consists only of exchange forces. The coupling among the states within each spin manifold should be stronger, because longer-range couplings, such as dipole coupling, can operate between states of the same spin. Two-state calculations for the excitation of the $b\,^3\Sigma_u^+$ state of H_2 have been carried out by several groups using a variety of *ab initio* theoretical methods and are in reasonably good accord with one another as well as with available experimental data.[9–12] Recently Lima *et al.*[6] extended these studies to look at excitation into the $a\,^3\Sigma_g^+$ and $c\,^3\Pi_u$ states, also within the two-state close-coupling model. However, the long-range dipole coupling between the a and c states leads one to question the validity of a two-state model for these excitation cross sections. Indeed, early calculations[13] on excitation of the $n=2$ states of helium, which is the atomic analog of H_2, showed that it is essential to include dipole coupling in the excited-state manifold in order to achieve meaningful excitation cross sections for excitation from the ground state.

To test this notion we have performed calculations on excitation at incident energies of up to 40 eV of the first three triplet excited states of H_2 ($b\,^3\Sigma_u^+$, $a\,^3\Sigma_g^+$, and $c\,^3\Pi_u$) by including all three excited states as well as the ground state in a close-coupling expansion. Comparison of results of our four-state calculations with two-state close-coupling calculations, involving only the ground and one excited state, reveals in some detail how coupling among electronically excited states qualitatively changes the simple two-channel picture. Comparison of the calculated differential cross sections with experimental re-

sults suggests the degree to which these calculations may be converged.

For the calculations reported here, we restricted ourselves to the use of simple target wave functions, each consisting of a single configuration. The $B\ ^1\Sigma_u^+$ state does not admit of such a simple description and was omitted, as were the $E,F\ ^1\Sigma_g^+$ and $C\ ^1\Pi_u$ states. The purpose of this paper is to examine the effects of long-range coupling between the triplet excited states and to obtain the cross sections for excitation of the a, b, and c states using single configuration descriptions of those states. Although a recent study[8] has reported the effect of excited-state coupling on the $b\ ^3\Sigma_u^+$ state cross section, a full set of excitation cross sections has not appeared previously. The calculations we present here are preparatory to a larger study involving six or more excited states that will include coupling to the singlet states involving the same orbitals as the triplets we have already included. In this study, we have concentrated on the intermediate energy region above 13 eV where all four channels are open. We do not report results below 13 eV here because this region is expected to be dominated by resonance structures that might be sensitive to the excited singlet states we have neglected.

In Sec. II we summarize the complex Kohn variational method as we have applied it in calculations on electron-molecule collisions. Section III describes the details of the calculation, and Sec. IV discusses our results and compares them with the other theoretical calculations and experiment.

II. COMPLEX KOHN VARIATIONAL METHOD IN e^--MOLECULE COLLISIONS

A complete description of the implementation of the complex Kohn variational[5] method to e^--molecule collisions is given elsewhere,[2,4] and therefore only a brief overview will be given here. We will employ atomic units in the equations which follow. We choose our trial wave function as

$$\Psi_{\Gamma_0}(r_1,r_2,r_3)=\sum_{\Gamma}\mathcal{A}(\chi_\Gamma(r_1,r_2)F_{\Gamma\Gamma_0}(r_3))+\sum_{\mu}d_\mu^{\Gamma_0}\Theta_\mu(r_1,r_2,r_3)\ , \tag{1}$$

where the first sum is only over open channels denoted by Γ. In Eq. (1) the target-state wave functions are χ_Γ, and the continuum functions are $F_{\Gamma\Gamma_0}$, describing an electron incident in channel Γ_0 and scattered into channel Γ. The second sum may include either closed-channel configurations and/or configurations to relax the orthogonality constraints discussed below. The continuum functions $F_{\Gamma\Gamma_0}$ are further expanded as

$$F_{\Gamma\Gamma_0}(\mathbf{r})=\sum_{l,m}[f_l^\Gamma(r)\delta_{ll_0}\delta_{mm_0}\delta_{\Gamma\Gamma_0}+T_{lml_0m_0}^{\Gamma\Gamma_0}g_l^\Gamma(r)]Y_{lm}(\hat{\mathbf{r}})/r+\sum_k c_k^{\Gamma\Gamma_0}\varphi_k^\Gamma(\mathbf{r})\ , \tag{2}$$

where $Y_{lm}(\hat{\mathbf{r}})$ is a spherical harmonic and $\varphi_k^\Gamma(\mathbf{r})$ denotes a square-integrable basis function, which, for this case, is a linear combination of Cartesian Gaussians. The continuum functions appearing in the expansion are defined in terms of regular, $j_l(kr)$, and irregular, $n_l(kr)$, Ricatti–Bessel functions according to

$$f_l^\Gamma(r)=\frac{h(r)j_l(k_\Gamma r)}{\sqrt{k_\Gamma}}\xrightarrow[r\to\infty]{}\frac{\sin(k_\Gamma r-l\pi/2)}{\sqrt{k_\Gamma}}\ ,$$
$$g_l^\Gamma(r)=\frac{ih(r)[j_l(k_\Gamma r)+in_l(k_\Gamma)c(r)]}{\sqrt{k_\Gamma}}\xrightarrow[r\to\infty]{}\frac{\exp[i(k_\Gamma r-l\pi/2)]}{\sqrt{k_\Gamma}}\ . \tag{3}$$

The functions $c(r)$ and $h(r)$ in Eq. (3) are cutoff functions with $c(r)$ chosen to regularize n_l at $r=0$ and $h(r)$ chosen to further exclude both the regular and irregular functions from the region of the target molecule. The cutoff functions are defined here to be

$$c(r)=(1-e^{-\alpha r})^{(2l+1)}\ ,$$
$$h(r)=(1-e^{-\gamma r})^n\ . \tag{4}$$

To complete the definition of the trial wave function, the channel momenta are given by

$$k_\Gamma=\sqrt{2(E-E_\Gamma)}\ . \tag{5}$$

In the trial wave function in Eq. (1) it is the T-matrix elements that are the objects of this effort, since they are the quantities from which both differential and integral scattering cross sections are constructed. These T-matrix elements are determined, using the Kohn principle, as the stationary value of the functional

$$[\underline{T}^{\Gamma\Gamma_0}]=\underline{T}^{\Gamma\Gamma_0}-2\int\Psi_\Gamma(H_{\text{eff}}-E)\Psi_{\Gamma_0}\ . \tag{6}$$

The parameters $T_{lml_0m_0}^{\Gamma\Gamma_0}$ and $c_k^{\Gamma\Gamma_0}$ are thus obtained from a set of linear equations that result from the requirement that the derivatives of Eq. (6) with respect to these parameters vanish. To cast the Kohn principle in this form, Feshbach partitioning is employed to define the effective Hamiltonian in Eq. (6):

$$H_{\text{eff}}=H_{PP}+(H-E)_{PQ}(E-H)_{QQ}^{-1}(H-E)_{QP}=H_{PP}+V_{\text{opt}}\ . \tag{7}$$

The Q space consists of the functions Θ_μ in Eq. (1) and thus the parameters $d_\mu^{\Gamma_0}$ need not be computed explicitly. The P space consists of the other terms in the trial wave function in Eq. (1).

The coefficients produced by the solution of the linear equations are then substituted back into Eq. (6) to yield the stationary value of the T matrix as

$$[\underline{T}]=-2(\underline{M}_{00}-\underline{M}_{q0}^t\underline{M}_{qq}^{-1}\underline{M}_{q0})\ . \tag{8}$$

Here $\underline{M}_{ij}$ is a matrix whose elements are obtained from

TABLE I. Exponents of Cartesian Gaussian basis in which the target states were expanded.

Center		Exponents
Hydrogen	s type	48.4479, 7.283 46, 1.651 39, 0.462 447, 0.145 885, 0.07
Hydrogen	p type	4.5, 1.5, 0.5, 0.25, 0.125, 0.031 25
Center	s type	0.25, 0.083, 0.027, 0.0093
Center	p type	0.19, 0.0655, 0.0226, 0.007 79

the operator $(H_{\text{eff}}-E)$. The subscript 0 denotes the subspace spanned by the functions $\{\chi_\Gamma f_l^\Gamma Y_{lm}\}$ and the subscript q denotes the subspace spanned by the functions $\{\chi_\Gamma g_l^\Gamma Y_{lm}\}$ and $\{\chi_\Gamma \varphi_k^\Gamma\}$. For example, a matrix element of $\underline{M}_{00}$ is defined by

$$(M_{00})^{\Gamma\Gamma_0}_{lml_0m_0} = \int \mathcal{A}(\chi_\Gamma f_l^\Gamma Y_{lm}) \times (H_{\text{eff}}-E)\mathcal{A}(\chi_{\Gamma_0} f_{l_0}^{\Gamma_0} Y_{l_0m_0}) \, . \quad (9)$$

Since g_l^Γ is defined to correspond to outgoing boundary conditions, the matrix $\underline{M}_{qq}$ is complex symmetric and generally has a nonsingular inverse when evaluated at real energies.[5,14,15]

The effort required to evaluate the matrix elements appearing in Eq. (8) determines the viability of the complex Kohn variational approach. In this regard several points need to be mentioned. First, the choice of Cartesian Gaussians as the basis in which both the target functions χ_Γ and the square-integrable portion of the continuum functions φ_k^Γ in Eqs. (1) and (2) are expanded, allows the use of standard electronic-structure methodology in the evaluation of the necessary bound-bound matrix elements. Second, orthogonalizing the continuum functions f_l^Γ and g_l^Γ to the square-integrable part of the scattering basis φ_k^Γ is allowed by a property of the Kohn principle called "transfer invariance," discussed in detail elsewhere.[16,17] In short, this property is that the T matrix remains unchanged by any unitary transformation among the basis functions. Additionally, by including "orthogonality relaxing" configurations in the Q space, the continuum functions can also be held orthogonal to the orbitals used to describe the target states. For example, if the continuum functions are orthogonalized to the $2\sigma_g$ orbital of the $(1\sigma_g 2\sigma_g)$ target state, then the configuration $(1\sigma_g 2\sigma_g^2)$ must be included in the Q space. Without the inclusion of these "orthogonality relaxing" configurations, the calculation would enforce an unphysical constraint on the total wave function. Third, the matrix elements of the optical potential V_{opt} as well as the exchange portions of the matrix elements in Eq. (7), are evaluated by approximating these operators with separable expansions.[18–20] For example, the exchange portion of H_{PP} is approximated by

$$H_{PP}^{\text{exch}} \approx \sum_{\substack{\Gamma,\Gamma_0 \\ k,k_0}} |\varphi_k^\Gamma \chi_\Gamma\rangle\langle\varphi_k^\Gamma \chi_\Gamma| H_{PP}^{\text{exch}} |\varphi_{k_0}^{\Gamma_0}\chi_{\Gamma_0}\rangle\langle\varphi_{k_0}^{\Gamma_0}\chi_{\Gamma_0}| \, . \quad (10)$$

In this approximation, matrix elements between bound functions are not changed but any exchange matrix element involving free functions vanishes by orthogonality. Finally, the direct matrix elements of H_{pp} involving continuum functions are evaluated by using a three-dimensional adaptive quadrature scheme discussed in detail elsewhere.[2]

III. COMPUTATIONAL PROCEDURES

A. Target states

The target states in Eq. (1) were obtained as follows. The ground state, $X\,^1\Sigma_g^+(1\sigma_g^2)$, wave function was calculated in the self-consistent-field (SCF) approximation in the basis described in Table I. The excited states, $b\,^3\Sigma_u^+$ $(1\sigma_g 1\sigma_u)$, $a\,^3\Sigma_g^+$ $(1\sigma_g 2\sigma_g)$, and $c\,^3\Pi_u$ $(1\sigma_g 1\pi_u)$, consist of single-configuration wave functions in which the molecular orbitals are expanded in the Gaussian basis described in Table I. The excited orbitals $(1\sigma_u$, $2\sigma_g$, and $1\pi_u)$ were determined in the V_{N-1} potential of H_2^+ with its electron in the H_2 $1\sigma_g$ orbital. All calculations were performed at the experimental equilibrium internuclear distance, $1.40a_0$. The SCF energy was $-1.133\,308$ hartrees and the V_{N-1} calculations lead to vertical excitation energies of 9.98, 12.03, and 12.31 eV for the $b\,^3\Sigma_u^+$, $a\,^3\Sigma_g^+$, and $c\,^3\Pi_u$ states, respectively. Accurate

TABLE II. Supplementary basis for expanding scattering functions in Eq. (2), augmenting basis in Table I.

Center		Exponents
Supplementary scattering		
Center	s type	0.0031, 0.001 03, 0.000 344
Center	p type	0.002 69, 0.000 926, 0.000 319
Center	d_{xy}, d_{xz}, and d_{yz} type	0.2, 0.08, 0.032, 0.0128
Center	d_{xy} type	0.005 12, 0.002 048, 0.000 819 2
Hydrogen	d_{xy} type	4.5, 1.8, 0.072, 0.0288, 0.011 52, 0.004 608

TABLE III. H_2 bound and continuum basis for $^2\Sigma_g^+$ and $^2\Sigma_u^+$ (see text for notation).

Target	P space		Q space
	$^2\Sigma_g^+$		
$X\,^1\Sigma_g^+$	$(1\sigma_g 1\sigma_g n\sigma_g)$ $n=3,\ldots$	$m=0$; $l=0,2,4,6$	$(1\sigma_g^2 2\sigma_g)$
$b\,^3\Sigma_u^+$	$(1\sigma_g 1\sigma_u n\sigma_u)$ $n=2,\ldots$	$m=0$; $l=1,3,5,7$	$(1\sigma_g 1\sigma_u^2)$
$a\,^3\Sigma_g^+$	$(1\sigma_g 2\sigma_g n\sigma_g)$ $n=3,\ldots$	$m=0$; $l=0,2,4,6$	$(1\sigma_g 2\sigma_g^2)$
$c\,^3\Pi_{uy}$	$(1\sigma_g 1\pi_{uy} n\pi_{uy})$ $n=2,\ldots$	$m=+1$; $l=1,3,5,7$	$(1\sigma_g 1\pi_{uy}^2)$
$c\,^3\Pi_{ux}$	$(1\sigma_g 1\pi_{ux} n\pi_{ux})$ $n=2,\ldots$	$m=-1$; $l=1,3,5,7$	$(1\sigma_g 1\pi_{ux}^2)$
	$^2\Sigma_u^+$		
$X\,^1\Sigma_g^+$	$(1\sigma_g 1\sigma_g n\sigma_u)$ $n=2,\ldots$	$m=0$; $l=1,3,5,7$	$(1\sigma_g^2 1\sigma_u)$
$b\,^3\Sigma_u^+$	$(1\sigma_g 1\sigma_u n\sigma_g)$ $n=3,\ldots$	$m=0$; $l=0,2,4,6$	$(1\sigma_g 1\sigma_u 2\sigma_g)$
$a\,^3\Sigma_g^+$	$(1\sigma_g 2\sigma_g n\sigma_u)$ $n=2,\ldots$	$m=0$; $l=1,3,5,7$	$(1\sigma_g 2\sigma_g 1\sigma_u)$
$c\,^3\Pi_{uy}$	$(1\sigma_g 1\pi_{uy} n\pi_{gy})$ $n=1,\ldots$	$m=+1$; $l=2,4,6,8$	
$c\,^3\Pi_{ux}$	$(1\sigma_g 1\pi_{ux} n\pi_{gx})$ $n=1,\ldots$	$m=-1$; $l=2,4,6,8$	

TABLE IV. H_2 bound and continuum basis for $^2\Pi_g$ and $^2\Pi_u$.

Target	P space		Q space
	$^2\Pi_{ux,y}$		
$X\,^1\Sigma_g^+$	$(1\sigma_g 1\sigma_g n\pi_{ux,y})$ $n=2,\ldots$	$m=-1$; $l=1,3,5,7$	$(1\sigma_g^2 1\pi_{ux,y})$
		$m=+1$; $l=1,3,5,7$	
$b\,^3\Sigma_u^+$	$(1\sigma_g 1\sigma_u n\pi_{gx,y})$ $n=1,\ldots$	$m=-1$; $l=2,4,6,8$	
		$m=+1$; $l=2,4,6,8$	
$a\,^3\Sigma_g^+$	$(1\sigma_g 2\sigma_g n\pi_{ux,y})$ $n=2,\ldots$	$m=-1$; $l=1,3,5,7$	$(1\sigma_g 2\sigma_g 1\pi_{ux,y})$
		$m=+1$; $l=1,3,5,7$	
$c\,^3\Pi_{uy}$	$(1\sigma_g 1\pi_{uy} n\sigma_g)$ $n=3,\ldots$	$m=0$; $l=0,2,4,6$	$(1\sigma_g 1\pi_{uy} 2\sigma_g)$
$c\,^3\Pi_{ux}$	$(1\sigma_g 1\pi_{ux} n\sigma_g)$ $n=3,\ldots$	$m=0$; $l=0,2,4,6$	$(1\sigma_g 1\pi_{ux} 2\sigma_g)$
	$^2\Pi_{gx,y}$		
$X\,^1\Sigma_g^+$	$(1\sigma_g 1\sigma_g n\pi_{gx,y})$ $n=1,\ldots$	$m=-1$; $l=2,4,6,8$	
		$m=+1$; $l=2,4,6,8$	
$b\,^3\Sigma_u^+$	$(1\sigma_g 1\sigma_u n\pi_{ux,y})$ $n=2,\ldots$	$m=-1$; $l=1,3,5,7$	$(1\sigma_g 1\sigma_u 1\pi_{ux,y})$
		$m=+1$; $l=1,3,5,7$	
$a\,^3\Sigma_g^+$	$(1\sigma_g 2\sigma_g n\pi_{gx,y})$ $n=1,\ldots$	$m=-1$; $l=2,4,6,8$	
		$m=+1$; $l=2,4,5,8$	
$c\,^3\Pi_{uy}$	$(1\sigma_g 1\pi_{uy} n\sigma_u)$ $n=2,\ldots$	$m=0$; $l=1,3,5,7$	$(1\sigma_g 1\pi_{uy} 1\sigma_u)$
$c\,^3\Pi_{ux}$	$(1\sigma_g 1\pi_{ux} n\sigma_u)$ $n=2,\ldots$	$m=0$; $l=1,3,5,7$	$(1\sigma_g 1\pi_{ux} 1\sigma_u)$

TABLE V. H_2 bound and continuum basis for $^2\Delta_{gxy}$ and $^2\Delta_{uxy}$.

Target	P space		Q space
	$^2\Delta_{gxy}$		
$X\,^1\Sigma_g^+$	$(1\sigma_g 1\sigma_g n\delta_{gxy})$ $n=1,\ldots$	$m=+2$; $l=2,4,6,8$	
$b\,^3\Sigma_u^+$	$(1\sigma_g 1\sigma_u n\delta_{uxy})$ $n=1,\ldots$	$m=+2$; $l=3,5,7,9$	
$a\,^3\Sigma_g^+$	$(1\sigma_g 2\sigma_g n\delta_{gxy})$ $n=1,\ldots$	$m=+2$; $l=2,4,6,8$	
$c\,^3\Pi_{uy}$	$(1\sigma_g 1\pi_{uy} n\pi_{ux})$ $n=2,\ldots$	$m=-1$; $l=1,3,5,7$	$(1\sigma_g 1\pi_{uy} 1\pi_{ux})$
$c\,^3\Pi_{ux}$	$(1\sigma_g 1\pi_{ux} n\pi_{uy})$ $n=2,\ldots$	$m=+1$; $l=1,3,5,7$	$(1\sigma_g 1\pi_{ux} 1\pi_{uy})$
	$^2\Delta_{uxy}$		
$X\,^1\Sigma_g^+$	$(1\sigma_g 1\sigma_g n\delta_{uxy})$ $n=1,\ldots$	$m=+2$; $l=3,5,7,9$	
$b\,^3\Sigma_u^+$	$(1\sigma_g 1\sigma_u n\delta_{gxy})$ $n=1,\ldots$	$m=+2$; $l=2,4,6,8$	
$a\,^3\Sigma_g^+$	$(1\sigma_g 2\sigma_g n\delta_{uxy})$ $n=1,\ldots$	$m=+2$; $l=3,5,7,9$	
$c\,^3\Pi_{uy}$	$(1\sigma_g 1\pi_{uy} n\pi_{gx})$ $n=1,\ldots$	$m=-1$; $l=2,4,6,8$	
$c\,^3\Pi_{ux}$	$(1\sigma_g 1\pi_{ux} n\pi_{gy})$ $n=1,\ldots$	$m=+1$; $l=2,4,6,8$	

values[21–23] of these excitation energies are 10.62, 12.54, and 12.93 eV.

B. Scattering basis, numerical details, and relaxing the orthogonality constraints

The scattering trial wave function is determined by specifying the square-integrable basis functions φ_k^Γ and the continuum basis in Eq. (2). The square-integrable basis functions were constructed in a basis formed by augmenting the target basis with the "supplementary functions" listed in Table II.

The scattering continuum functions were chosen to be those corresponding to the first four lm pairs that contribute to the symmetry of the appropriate scattered wave as indicated in Tables III–V. For example, in the $^2\Sigma_g^+$ symmetry component, the ground state $X\,^1\Sigma_g^+$ $(1\sigma_g^2)$ is combined with the $n\sigma_g$ scattering orbitals, and the continuum functions correspond to the lm pairs with $m=0$ and $l=0,2,4,6$. We chose the cutoff parameters, which complete the definition of the continuum functions f_l^Γ and g_l^Γ in Eqs. (2)–(4), to be $\alpha=1.0$, $\gamma=1.0$, and $n=0$. In Tables III–V the entries under the heading "Q space" indicate orbital occupancies. All spin couplings leading to an overall doublet are included.

As a test of the numerical parameters (grid, continuum basis, etc.) of our Kohn variational calculations, and to assure ourselves that the final results do not depend on our choice of Gaussian basis, we performed a series of two-channel calculations. We first used a basis of Gaussian functions identical to that employed by Lima *et al.*[6] For the $b\,^3\Sigma_u^+$ state we obtained results that agreed to within 5% with both the linear algebraic and Kohn variational calculations of Schneider and Rescigno.[1] We then employed the larger basis set in Table II, and the results of those calculations agreed (for all transitions from the ground state) with the results from the smaller basis set to within 3%. However, our results for the b and c states at this level agreed to within 10% with those of Lima *et al.*,[6] and only within 25% for the a state. We speculate that the discrepancies between the present results and those of Lima *et al.*[6] are due to their method of computing free-free matrix elements of the Green's function in their calculations. These authors have since developed a more sophisticated method for calculating these matrix elements.[24]

IV. RESULTS AND DISCUSSION

As mentioned previously, our calculations differ from the two-channel calculations of Lima *et al.*[6] in that the three excited states ($b\,^3\Sigma_u^+$, $a\,^3\Sigma_g^+$, and $c\,^3\Pi_u$ are allowed to couple among themselves as well as with the ground state ($X\,^1\Sigma_g^+$). One would expect this coupling to be strong, since transitions between the $a\,^3\Sigma_g^+$ and $c\,^3\Pi_u$ states as well as between the $a\,^3\Sigma_g^+$ and $b\,^3\Sigma_u^+$ states are dipole allowed. The effects of this coupling can be seen in a comparison of the cross sections for the $a\,^3\Sigma_g^+$ and $c\,^3\Pi_u$ channels in the two-channel calculations of Lima *et al.*[6] with those of the present calculations shown in Figs. 1–3. Figure 1 shows that the integral cross section for

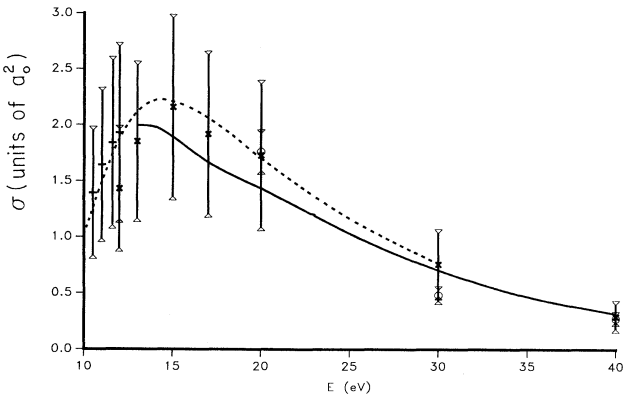

FIG. 1. The integral cross section for the $X\,^1\Sigma_g^+$ to $b\,^3\Sigma_u^+$ channel. The solid curve is the present results; dashed curve the results of Lima *et al.* (Ref. 6); +: experimental results of Hall and Andric, (Ref. 26); ×: experimental results of Nishimura and Danjo (Ref. 27); ○: experimental results of Khakoo *et al.* (Ref. 28).

excitation from the ground state to the $b\,^3\Sigma_u^+$ state is relatively unchanged by coupling of the excited states, whereas the integral cross sections for the $a\,^3\Sigma_g^+$ and $c\,^3\Pi_u$ channels in Figs. 2 and 3 show a significant change from the two-channel results. We observe the apparent transfer of flux from the $c\,^3\Pi_u$ to the $a\,^3\Sigma_g^+$ channels in the energy range from threshold to about 30 eV.

This effect is primarily a result of the differences in relative importance of the various symmetry contributions to the total cross section between a two-channel calculation and a four-channel calculation. For example, in a two-channel calculation including only the ground state and the $a\,^3\Sigma_g^+$ state, the contribution from the $^2\Delta_g$ symmetry is negligible, and the calculation is found to be con-

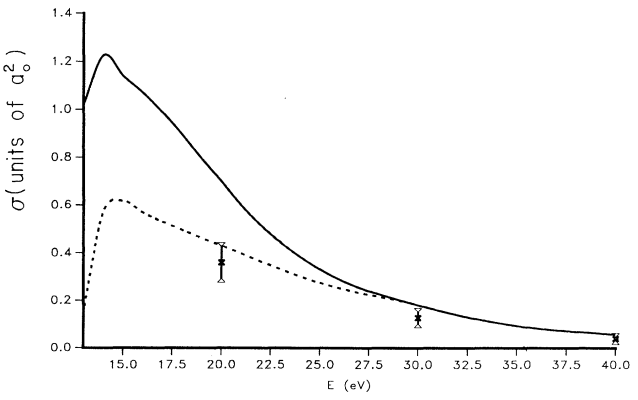

FIG. 2. The integral cross section for the $X\,^1\Sigma_g^+$ to $a\,^3\Sigma_g^+$ channel. The solid curve is the present results; dashed curve the results of Lima *et al.* (Ref. 6); ×, experimental results of Khakoo and Trajmar (Ref. 29).

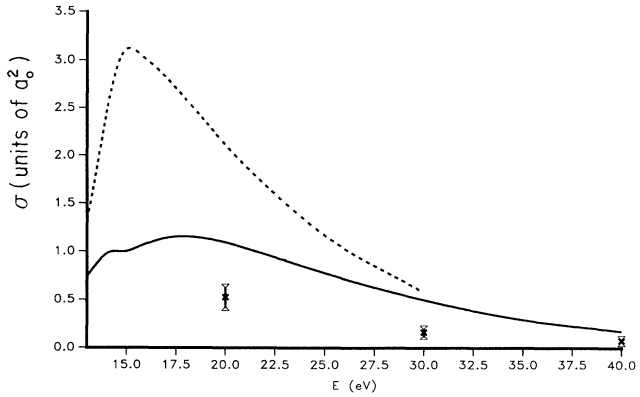

FIG. 3. As in Fig. 2, for the $X\ ^1\Sigma_g^+$ to $c\ ^3\Pi_u$ channel.

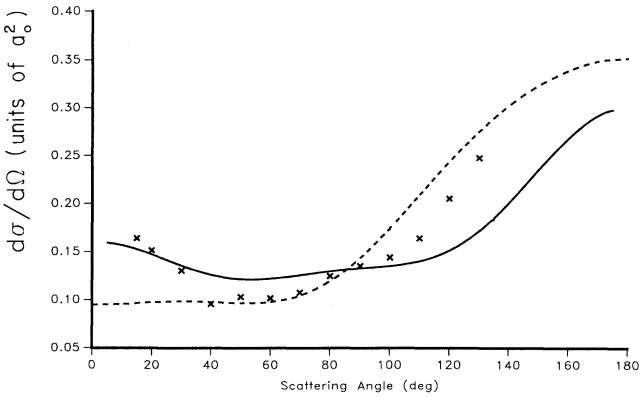

FIG. 5. As in Fig. 4, for the $b\ ^3\Sigma_u^+$ state at 15 eV.

verged with respect to angular momentum contributions with inclusion of only the four symmetry contributions $^2\Sigma_g^+$, $^2\Sigma_u^+$, $^2\Pi_g$, and $^2\Pi_u$. However, upon coupling of the three excited states, the contribution of the $^2\Delta_g$ symmetry to the $a\ ^3\Sigma_g^+$ cross section becomes as important as the $^2\Sigma_g^+$ contribution. In the analogous He $2\ ^3S$ excitation cross section, the $L=2$ total angular momentum contribution is also large.[25] We also find that the importance of the $^2\Pi_g$ and $^2\Pi_u$ symmetry contributions grow at the expense of the $^2\Sigma_u^+$ symmetry contribution in the four-channel calculations.

Differential cross sections for excitation of the a, b, and c states are compared with experiment[26–29] in Figs. 4–9. The increase in the relative importance of the $^2\Delta_g$ symmetry contribution has a marked effect on the differential cross section for the excitation into the $a\ ^3\Sigma_g^+$ state, as is shown in Fig. 7. Here we note the striking similarity between the differential cross sections for the excitation of H_2 from its ground state $X\ ^1\Sigma_g^+$ to the excited state $a\ ^3\Sigma_g^+$ and for the excitation of He from its ground state $1\ ^2S$ to the excited state $2\ ^3S$ (Ref. 30) (the united-atom limit of H_2 in $a\ ^3\Sigma_g^+$). We note here that the experimental He points given for 0°, 160°, and 180° were obtained by extrapolation.[30] From these results it appears that coupling between the excited states is necessary to describe the apparent double minimum feature of the differential cross section in the $a\ ^3\Sigma_g^+$ cross section. We find that the discrepancy between the experimental values for the total cross section for the excitation into the $a\ ^3\Sigma_g^+$ state and our theoretical results is due to contributions from scattering near 0° and 180° where no measurements were made (see Fig. 6). Khakoo and Trajmar[29] state that they used available theoretical data "as a guide" in extrapolating their differential cross sections into these regions for the purpose of computing total cross sections. The fact that our cross sections for the $a\ ^3\Sigma_g^+$ state are larger than the earlier results of Lima *et al.*[6] beyond 120°, where no direct measurements were made, may thus be partly responsible for the larger values of the total cross section that we find. For scattering angles below 30°, however,

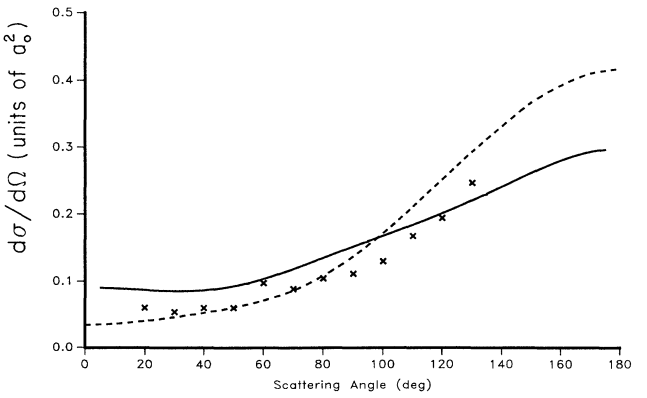

FIG. 4. Differential cross sections for excitation to the $b\ ^3\Sigma_u^+$ state at 13 eV. The solid curve is the present results; dashed curve the results of Lima *et al.* (Ref. 6); ×: experimental results of Nishimura and Danjo (Ref. 27).

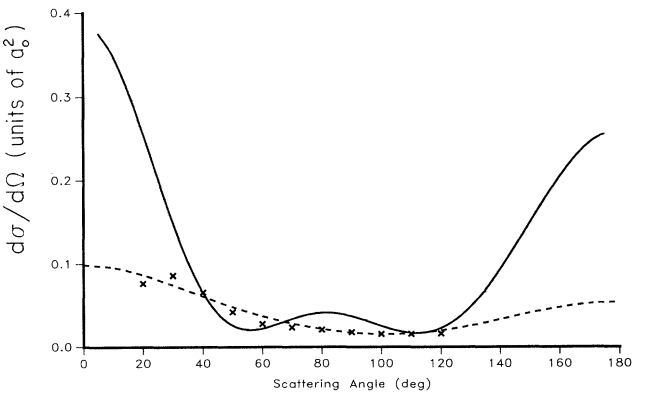

FIG. 6. Differential cross sections for excitation to the $a\ ^3\Sigma_g^+$ state at 20 eV. The solid curve is the present results; dashed curve the results of Lima *et al.* (Ref. 6); ×: experimental results of Khakoo and Tramjar (Ref. 29).

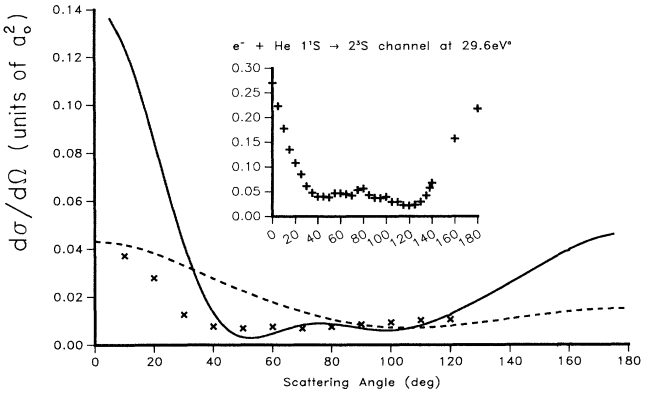

FIG. 7. As in Fig. 6, for the $a\ ^3\Sigma_g^+$ state at 30 eV. (a) The inset contains a differential cross section for excitation of the He $2\ ^3S$ state (Ref. 30) adjusted to units of square Bohr for comparison with present results. Note that the experimental He points given for 0°, 160°, and 180° were obtained by Khakoo and Trajmar (Ref. 29) by extrapolating their experimental results.

our $a\ ^3\Sigma_g^+$ cross sections are larger than both the experimental results of Khakoo and Trajmar[29] and the two-state results of Lima *et al.*[6] As we stated previously, the sharp forward and backward peaks in our $a\ ^3\Sigma_g^+$ differential cross section are caused by the strong contribution from $^2\Delta_g$ symmetry, which only comes about from the coupling between the $a\ ^3\Sigma_g^+$ and $c\ ^3\Pi_u$ states and is hence not evident in the two-state results of Lima *et al.*[6] It is possible that more elaborate target wave functions and the inclusion of more excited states would modify these results to some extent. We are currently investigating these questions.

Comparison of the other excited states of H_2 with their analogous, united-atom limit He excited states is less straightforward since the $2\ ^3P$ state of He has three components x, y, and z. The z component maps onto the $b\ ^3\Sigma_u^+$ state of H_2 and the x and y components map onto

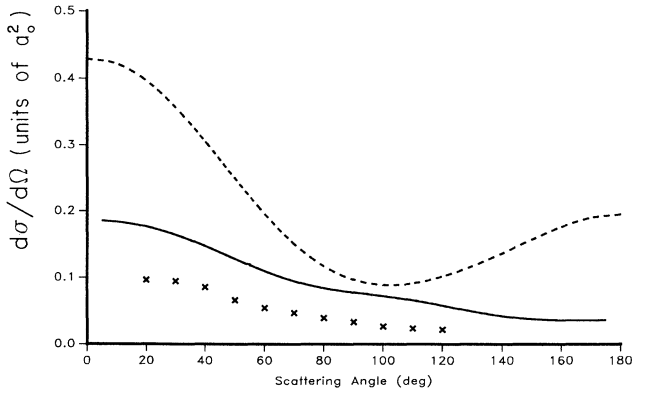

FIG. 8. As in Fig. 6, for the $c\ ^3\Pi_u$ state at 20 eV.

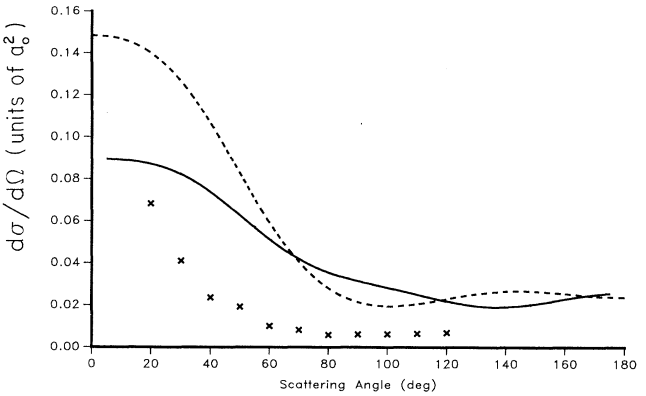

FIG. 9. As in Fig. 6, for the $c\ ^3\Pi_u$ state at 30 eV.

the x and y components of the $c\ ^3\Pi_u$ state. However, the differential cross sections for the excitation of the $2\ ^3P$ state is fairly isotropic as are those of the H_2 b and c states.

Before concluding, we would like to comment on a subtle aspect of these calculations. We eliminate the orthogonality constraints on the scattering wave function by the inclusion of appropriate Q space configurations. However, these configurations can also couple to open channels not explicitly included in the close-coupling expansion. For example, the configuration $(1\sigma_g 1\sigma_u^2)$ relaxes the constraint that the continuum function be orthogonal to the $1\sigma_u$ orbital used in the $b\ ^3\Sigma_u^+$ target state. However, this configuration, which couples both to the $b\ ^3\Sigma_u^+$ and $B\ ^1\Sigma_u^+$ states, is precisely the one that would be included in a calculation including the $B\ ^1\Sigma_u^+$ state explicitly. Effects such as this have recently been discussed by da Silva *et al.*[7] and by Branchett and Tennyson[8] and clearly point out a need for more extensive calculations in which all of the low-lying electronic states are included.

In summary, the strong dipole coupling between the a, b, and c states of H_2 dictates that all of these states be included in close-coupling electron-impact-excitation calculations. These calculations also have highlighted the similarity between excitations in H_2 and analogous processes in He.[30] In addition, the differential cross sections obtained in our four-channel calculations were found to be in good agreement with experiment in the angular regions in which measurements have been made.[26–29] Based on the similarity of these calculations with earlier experimental and theoretical studies of He and on the comparison of our differential cross sections with available experimental results, we believe the integral cross sections we obtain for electron-impact excitation from the ground state of H_2 to the $a\ ^3\Sigma_g^+$ and $c\ ^3\Pi_u$ states to be the most reliable theoretical cross sections yet to appear. We also wish to emphasize the importance of considering dipole coupling among the excited states in the design of electron-impact calculations in which a limited number of open channels are included in the close-coupling expansion.

ACKNOWLEDGMENT

The work at Ohio State University was supported by National Science Foundation Grant No. CHE-8922836, and by a grant of time from the Ohio Supercomputer Center. The work at the Lawrence Livermore National Laboratory was performed under the auspices of the U.S. Department of Energy under Contract No. W-7405-ENG-48.

[1]B. I. Schneider and T. N. Rescigno, Phys. Rev. A **37**, 3749 (1988).
[2]C. W. McCurdy and T. N. Rescigno, Phys. Rev. A **39**, 4487 (1989).
[3]T. N. Rescigno, C. W. McCurdy, and B. I. Schneider, Phys. Rev. Lett. **63**, 248 (1989).
[4]T. N. Rescigno, B. H. Lengsfield III, and C. W. McCurdy, Phys. Rev. A **41**, 2462 (1990).
[5]W. H. Miller and B. M. D. D. Jansen op de Haar, Phys. Rev. A **36**, 2061 (1987).
[6]M. A. P. Lima, T. L. Gibson, V. McKoy, and W. M. Huo, Phys. Rev. A **38**, 4527 (1988).
[7]A. J. R. da Silva, M. A. P. Lima, L. M. Brescansin, and V. McKoy, Phys. Rev. A **41**, 2903 (1990).
[8]S. E. Branchett and J. Tennyson, Phys. Rev. Lett. **64**, 2889 (1990).
[9]K. L. Beluja, C. J. Noble, and J. Tennyson, J. Phys. B **18**, L851 (1985).
[10]B. I. Schneider and L. A. Collins, J. Phys. B **18**, L857 (1985).
[11]M. A. P. Lima, T. L. Gibson, C. C. Lin, and V. McKoy, J. Phys. B **18**, L865 (1985).
[12]T. N. Rescigno and B. I. Schneider, J. Phys. B **21**, L691 (1988).
[13]H. S. W. Massey and E. H. S. Burhop, *Electronic and Ionic Impact Phenomena* (Oxford University Press, New York, 1969), Vol. 1, p. 549.
[14]C. W. McCurdy, T. N. Rescigno, and B. I. Schneider, Phys. Rev. A **36**, 2061 (1987).
[15]R. R. Lucchese, Phys. Rev. A **40**, 6879 (1989).
[16]T. N. Rescigno and B. I. Schneider, Phys. Rev. A **37**, 1044 (1988).
[17]R. K. Nesbet, *Variational Methods in Electron-Atom Scattering* (Plenum, New York, 1980).
[18]B. I. Schneider and L. A. Collins, Phys. Rev. A **24**, 1264 (1981).
[19]T. N. Rescigno and A. E. Orel, Phys. Rev. A **23**, 1134 (1981).
[20]T. N. Rescigno and A. E. Orel, Phys. Rev. A **24**, 1267 (1981).
[21]W. Kolos and L. Wolniewicz, J. Chem. Phys. **43**, 2429 (1965).
[22]W. Kolos and L. Wolniewicz, J. Chem. Phys. **48**, 3672 (1968).
[23]J. C. Browne, J. Chem. Phys. **40**, 43 (1964). The energy for the $c\,^3\Pi_u$ state at $1.4a_0$ was obtained by quadratic fit to three points at $1.0a_0$, $1.5a_0$, and $1.75a_0$.
[24]M. A. P. Lima, L. M. Brescansin, A. J. R. da Silva, C. Winstead, and V. McKoy, Phys. Rev. A **41**, 327 (1990).
[25]P. G. Burke, J. W. Cooper, and S. Ormond, Phys. Rev. **183**, 245 (1969).
[26]R. I. Hall and L. Andric, J. Phys. B **17**, 3815 (1984).
[27]H. Nishimura and A. Danjo, J. Phys. Soc. Jpn. **55**, 3031 (1986).
[28]M. A. Khakoo, S. Trajmar, R. McAdams, and T. W. Shyn, Phys. Rev. A **35**, 2832 (1987).
[29]M. A. Khakoo and S. Trajmar, Phys. Rev. A **34**, 146 (1986).
[30]S. Trajmar, Phys. Rev. A **8**, 191 (1973).